Available online at www.sciencedirect.com
ScienceDirect
Ceramics International 38S (2012) S83–S86
CERAMICS INTERNATIONAL
www.elsevier.com/locate/ceramint

Preparation and ferroelectric properties of $(Na_{0.5}Bi_{0.5})_{0.94}Ba_{0.06}TiO_3$ thin films deposited on Pt electrodes using $LaNiO_3$ as buffer layer

Xiao-lei Fang, Bo Shen, Ji-wei Zhai *, Xi Yao

Functional Materials Research Laboratory, Tongji University, 1239 Siping Road, Shanghai 200092, China

Available online 30 April 2011

Abstract

$(Na_{0.5}Bi_{0.5})_{0.94}Ba_{0.06}TiO_3$ thin films were deposited on Pt/Ti/SiO_2/Si (1 1 1) and $LaNiO_3$/Pt/Ti/SiO_2/Si (1 1 1) substrates by a sol–gel process. The phase structure and ferroelectric properties were investigated. The X-ray diffraction pattern indicated that the $(Na_{0.5}Bi_{0.5})_{0.94}Ba_{0.06}TiO_3$ thin film deposited on Pt/Ti/SiO_2/Si (1 1 1) substrates is polycrystalline structure without any preferred orientation. But the thin film deposited on $LaNiO_3$/Pt/Ti/SiO_2/Si substrates shows highly (1 0 0) orientation ($f \geq 81\%$). The leakage current density for the two thin films is about 6×10^{-3} A/cm^2 at 250 kV/cm, and thin film deposited on $LaNiO_3$/Pt/Ti/SiO_2/Si substrates possessed a much lower leakage current under high electric field. The hysteresis loops at an applied electric field of 300 kV/cm and 10 kHz were acquired for the thin films. The thin films deposited on $LaNiO_3$/Pt/Ti/SiO_2/Si substrates showed improved ferroelectricity.
© 2011 Elsevier Ltd and Techna Group S.r.l. All rights reserved.

Keywords: NBT-BT; Thin film; Buffer layer; Ferroelectric properties

1. Introduction

Lead-based ferroelectric materials represented by $PbTiO_3$ and Pb(Zr, Ti)O_3 are widely used due to their excellent ferroelectric and piezoelectric properties. However, lead toxicity is a tremendous disadvantage to the environment. Inevitably, developing lead-free materials is of great importance. Sodium bismuth titanate $Na_{0.5}Bi_{0.5}TiO_3$ (NBT) is considered to be one of the promising materials since it was discovered by Smolenski et al. [1]. Bulk ceramics of NBT have shown strong ferroelectricity at room temperature (remnant polarization $P_r = 38$ μC/cm^2 and coercive field $E_c = 73$ kV/cm) with a relative high Curie temperature of 320 °C. NBT-based bulk ceramics modified with $BaTiO_3$ (BT) show improved properties due to the existence of rhombohedral–tetragonal morphotropic phase boundary (MPB) [2,3]. The piezoelectric constant d_{33} of the NBT-BT ceramics with the MPB composition can reach up to 125 pC/N [4], and the (1 0 0)-oriented crystals grown by spontaneous nucleation method showed a piezoelectric constant of $d_{33} = 450$ pC/N and electric field induced strain up to 0.25% [5]. Also, for MPB composition, some researchers got bulk ceramics with pyroelectric coefficient $Pi = 3.9 \times 10^{-4}$ cm^{-2} K^{-1} [6], which possibly resulted from the large spontaneous and remnant polarization ($P_r = 40$ μC/cm^2) and lower depolarization temperature ($T_d = 100$ °C) [4]. However, NBT-BT in the form of thin films has rarely been studied because the existence of precipitation when adding BT to NBT. Recently, we use ammonia solution to stabilize the solution. Meanwhile, buffer layers are widely used to improve the properties of the thin films, such as $LaNiO_3$ and $NaNbO_3$ [7–9]. $LaNiO_3$ (LNO) has a pseudo cubic perovskite structure ($a = 3.84$ Å), which is not only a good candidate for the electrode material due to its good metallic conductivity, but also a promising buffer layer material for oriented growth.

2. Experimental

Two solutions were fabricated with nominal compositions of $Na_{0.5}Bi_{0.5}TiO_3$ (NBT) and $BaTiO_3$ (BT), respectively.

The NBT sol was synthesized first. Sodium acetate, $CH_3COONa{\cdot}3H_2O$, bismuth nitrate, $Bi(NO_3)_3{\cdot}5H_2O$, were mixed and stirred in acetic acid at 70 °C for 120 min, which was denoted as sol 1. On the other hand, acetylacetone ($CH_3COCH_2COCH_3$) was mixed with 2-methoxyethanol,

* Corresponding author. Tel.: +86 21 65980544; fax: +86 21 65985179.
E-mail address: apzhai@tongji.edu.cn (J.-w. Zhai).

0272-8842/$36.00 © 2011 Elsevier Ltd and Techna Group S.r.l. All rights reserved.
doi:10.1016/j.ceramint.2011.04.055

stirred for 30 min, and we added titanium tetra-n-butyl into the mixture. The mixture was stirred constantly until a transparent solution was obtained. We denoted this sol as sol 2. Sol 1 and sol 2 were mixed and control the concentration to 0.3 M by adding acetic acid. After stirring for 60 min, NBT sol was prepared.

Barium acetate, $Ba(CH_3COO)_2$, was dissolved in acetic acid at 70 °C for 30 min, which was denoted as sol 3. Meanwhile, we made sol 4 using the same method of sol 2. Thereafter, sol 3 and sol 4 were mixed and stirred for 60 min. We control the concentration to 0.3 M by adding acid.

Proper amounts of NBT and BT were mixed and we added ammonia water until it became transparent. After stirring for 60 min, NBT-BT sol was prepared, and the concentration will be adjusted to 0.3 M by adding acid. The flow chart of the synthesis process of the precursor solution is shown in Fig. 1.

There are two kinds of substrates used in this study, Pt/Ti/SiO_2/Si (1 1 1) and $LaNiO_3$/Pt/Ti/SiO_2/Si (1 1 1) substrates. The LNO layer was prepared by magnetron sputtering on Pt/Ti/SiO_2/Si (1 1 1) and the substrate temperature was kept at 300 °C. The LNO film exhibited a single perovskite phase with strong (1 0 0) orientation. The NBT-BT solutions were deposited on the two substrates by spin-coating at 3000 rpm for 20 s, respectively. After spin-coating, the gel layers were dried at 400 °C for 10 min. The spin-coating and heat-treatment process were repeated several times to obtain the desired thickness. Finally, the films were annealed at 700 °C for 30 min.

The crystalline phase of the films was determined by X-ray diffraction (BRUKER D8, Germany). The surface morphology was identified by FESEM (FEI Quanta 200 FEG). For electrical measurements of a metal/insulator/metal (MIM) structure, gold electrode pads of 500 μm in diameter were prepared through a shadow mask by DC-sputtering. The capacitance–voltage and capacitance–frequency characteristics were measured using an Agilent 4980A LCR meter. The leakage current–voltage characteristics were measured using a Keithley 6517A. The hysteresis loops were acquired by a ferroelectric test system (Radiant Precision Premier Π).

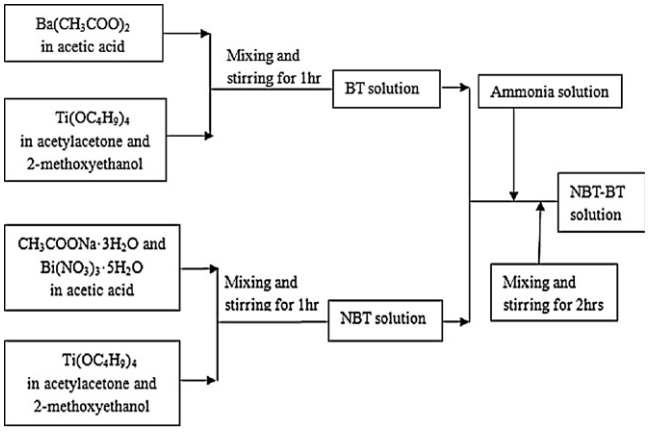

Fig. 1. Flow chart of preparation process of NBT-BT solutions.

3. Results and discussion

Fig. 2 shows the XRD patterns of the NBT-BT thin films deposited on Pt/Ti/SiO_2/Si (1 1 1) and LNO/Pt/Ti/SiO_2/Si (1 1 1) substrates. The XRD patterns indicated that the thin film deposited on Pt/Ti/SiO_2/Si substrates is polycrystalline structure. But, films deposited on LNO/Pt/Ti/SiO_2/Si substrates showed a highly preferred orientation of (1 0 0). The degree of grain orientation can be calculated by Lotgering factor f, which is defined as [10]

$$f = \frac{p - p_0}{1 - p_0} \tag{1}$$

where

$$p = \frac{\sum_i I(h\,0\,0)}{\sum_i I(h\,k\,l)} \tag{2}$$

$$p_0 = \frac{\sum_i I(h\,0\,0)}{\sum_i I(h\,k\,l)} \tag{3}$$

and $\sum_i I(h\ 0\ 0)$ is the sum of the (h 0 0) peak intensities for the sample, $\sum_i I(h\ k\ l)$ is the sum of all peak intensities in the sample diffraction pattern, while the data for p_0 are the parameters provided by the standard PDF cards. The orientation degree of NBT-BT thin film deposited on LNO/Pt/Ti/SiO_2/Si substrates is 81%, whereas the value for the other is only 40%. Based on the XRD results, we can contribute the highly (1 0 0) orientation to the good lattice match between NBT-BT and LNO buffer layer. Only series of NBT-BT peaks were observed, suggesting that there is no second phase in these films. The peaks are sharp, indicating that the thin films are well crystallized.

Fig. 3(a) indicates that the thin film deposited on LNO/Pt/Ti/SiO_2/Si substrates is crack-free, uniform and in a dense form. While the thin film deposited on Pt/Ti/SiO_2/Si substrates is also crack-free, but it has some pores, as shown in Fig. 3(b), which may affect the properties of the thin film.

The dielectric constant and loss tan δ were measured as function of voltage and frequency at room temperature, respectively, as shown in Figs. 4 and 5. The electric field is

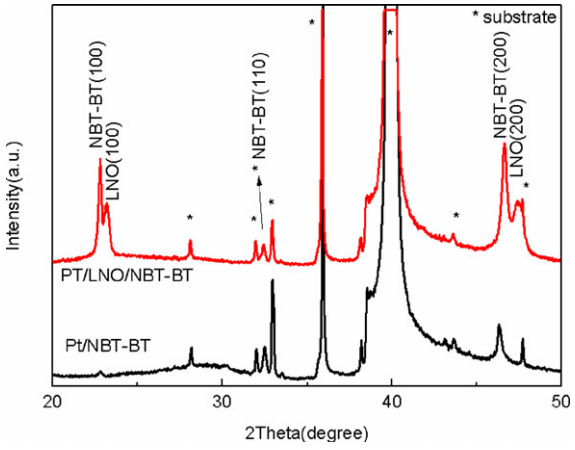

Fig. 2. XRD patterns of NBT-BT thin films deposited on Pt/Ti/SiO_2/Si (1 1 1) and LNO/Pt/Ti/SiO_2/Si (1 1 1) substrates.

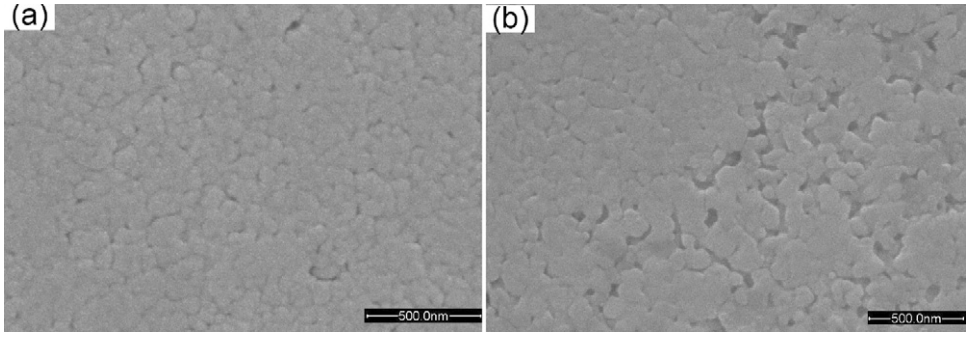

Fig. 3. FESEM images of NBT-BT thin films deposited on (a) LNO/Pt/Ti/SiO_2/Si (1 1 1) substrates and (b) Pt/Ti/SiO_2/Si (1 1 1) substrates.

applied as follows: 300 → 0 → −300 → 0 → 300 kV/cm. The *C–V* curve shows strong non-linear dielectric behavior. As shown in Fig. 4, the dielectric constant of NBT-BT thin film deposited on Pt/Ti/SiO_2/Si substrates was higher, and the dielectric loss was lower as well. The largest dielectric constant (ε_r) value is obtained by applying the electric field in a direction vertical to the polarization direction and the smallest ε_r value is obtained when the direction of the applied electric field is parallel to the polarization direction [11]. Considering the preferred orientation of NBT-BT thin film deposited on LNO/Pt/Ti/SiO_2/Si substrates is (1 0 0), we got the smallest ε_r, which is smaller than the film without any preferred orientation. Meanwhile, there is a slight asymmetry observed in the *C–V* curves, suggesting that the thin films contain movable ions or charges accumulated at the interface between the film and the electrodes. The dielectric constant and loss are about 630 and 0.03 at 10 kHz at room temperature for the thin film deposited on Pt/Ti/SiO_2/Si substrates, while the values are 450 and 0.06 for the other film.

In addition to the dielectric properties, the leakage current characteristics are also very important. In this study, the current–voltage measurements were conducted in metal–insulator–metal (MIM) configuration. As shown in Fig. 6, the leakage current density is about 6×10^{-3} A/cm^2 at 250 kV/cm and an abrupt increasing trend is observed at higher electric field for the films deposited on Pt/Ti/SiO_2/Si substrates. Under the electric field of 400 kV/cm, NBT-BT film deposited on LNO/Pt/Ti/SiO_2/Si substrates showed a much lower leakage current, nearly 1/5 of the film deposited on Pt/Ti/SiO_2/Si substrates. From Fig. 3(b), we can see some pores, and the pores may lead to the high leakage current under high electric field. The NBT-BT film deposited on Pt/Ti/SiO_2/Si substrates may have more oxygen vacancies trapped at the grain boundaries that can pin domains and result in the high leakage current as well as the low dielectric loss [12,13].

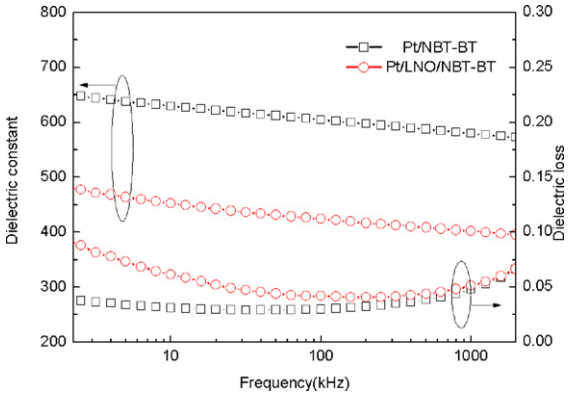

Fig. 5. Dielectric constant and loss tan δ as function of frequency of the NBT-BT thin films deposited on Pt/Ti/SiO_2/Si (1 1 1) and LNO/Pt/Ti/SiO_2/Si (1 1 1) substrates.

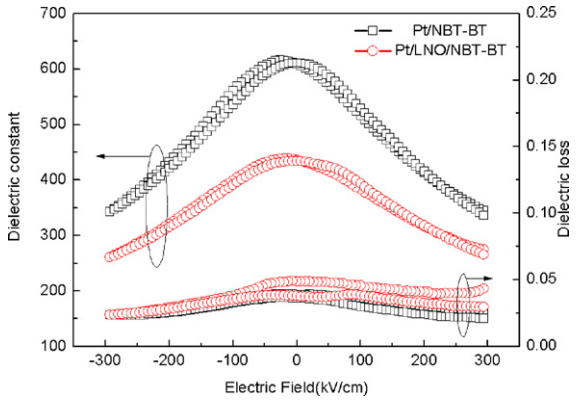

Fig. 4. Dielectric constant and loss tan δ as function of applied electric field of NBT-BT thin films deposited on Pt/Ti/SiO_2/Si (1 1 1) and LNO/Pt/Ti/SiO_2/Si (1 1 1) substrates.

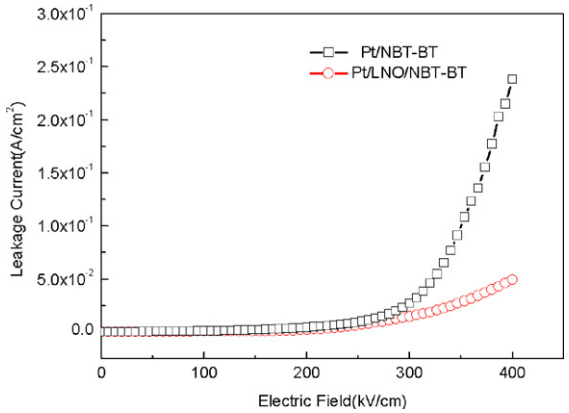

Fig. 6. *J–E* curve of NBT-BT thin films deposited on Pt/Ti/SiO_2/Si (1 1 1) and LNO/Pt/Ti/SiO_2/Si (1 1 1) substrates.

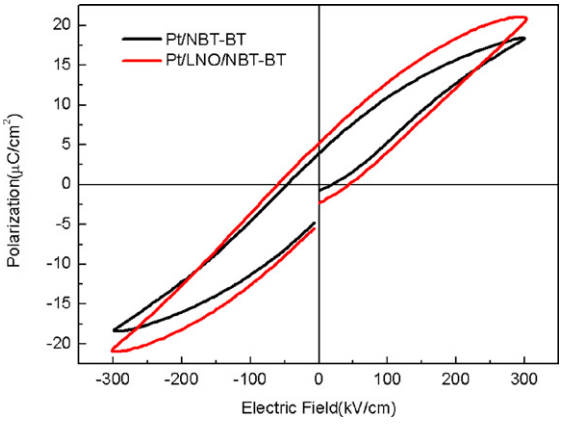

Fig. 7. *P–E* loops of the NBT-BT thin films deposited on Pt/Ti/SiO_2/Si (1 1 1) and LNO/Pt/Ti/SiO_2/Si (1 1 1) substrates.

Fig. 7 shows the hysteresis loops of the thin films. The hysteresis loops at an applied electric field of 300 kV/cm and 10 kHz were acquired for NBT-BT films deposited on Pt/Ti/SiO_2/Si substrates (saturation polarization $P_s \sim 18\ \mu C/cm^2$, remnant polarization $2P_r \sim 7.5\ \mu C/cm^2$ and coercive field $2E_c \sim 70$ kV/cm). Meanwhile, the hysteresis loops for NBT-BT films deposited on LNO/Pt/Ti/SiO_2/Si substrates were also acquired at the same condition. There was an increase of the coercive field ($2E_c \sim 100$ kV/cm). But the saturation polarization is bigger ($P_s \sim 21\ \mu C/cm^2$) and the remnant polarization was 40% larger ($2P_r \sim 11\ \mu C/cm^2$), which may derive from the preferred orientation and better crystallinity of the thin film as shown in Figs. 2 and 3 [14].

4. Conclusions

$(Na_{0.5}Bi_{0.5})_{0.94}Ba_{0.06}TiO_3$ thin films were deposited on Pt/Ti/SiO_2/Si (1 1 1) and LNO/Pt/Ti/SiO_2/Si (1 1 1) substrates by a sol–gel process. The X-ray diffraction pattern indicated that the NBT-BT thin film deposited on Pt/Ti/SiO_2/Si (1 1 1) substrates is polycrystalline structure without any preferred orientation. But the NBT-BT thin film deposited on LNO/Pt/Ti/SiO_2/Si substrates shows highly (1 0 0) orientation. NBT-BT thin film deposited on LNO/Pt/Ti/SiO_2/Si substrates possessed a much lower leakage current, nearly 1/5 of the NBT-BT film deposited on Pt/Ti/SiO_2/Si substrates under 400 kV/cm. There was an increase of the coercive field for the NBT-BT films deposited on LNO/Pt/Ti/SiO_2/Si substrates. But P_s and $2P_r$ is about 21 $\mu C/cm^2$ and 11 $\mu C/cm^2$, and are much bigger than that of thin film deposited on Pt/Ti/SiO_2/Si.

Acknowledgement

The authors would like to acknowledge the support from the National Natural Science Foundation of China under grant Nos. 50972108 and 50932007.

References

[1] G.A. Smolenski, V.A. Isupov, A.I. Agranovskaya, N.N. Krainik, New ferroelectrics of complex composition IV, Soviet Physics Solid State 2 (1961) 2651–2654.
[2] M.S. Yoon, N.H. Khansur, B.K. Choi, Y.G. Lee, S.C. Ur, The effect of nano-sized BNBT on microstructure and dielectric/piezoelectric properties, Ceramics International 35 (2009) 3027–3036.
[3] B.J. Chu, D.R. Chen, G.R. Li, Q.R. Yin, Electrical properties of $Na_{0.5}Bi_{0.5}TiO_3$–$BaTiO_3$ ceramics, Journal of the European Ceramic Society 22 (2002) 2115–2121.
[4] T. Takenaka, K. Maruyama, K. Sakata, $(Bi_{(1/2)}Na_{(1/2)})TiO_3$–$BaTiO_3$ system for lead-free piezoelectric ceramics, Japanese Journal of Applied Physics 30 (1991) 2236–2239.
[5] Y.M. Chiang, G.W. Farrey, A.N. Soukhojak, Lead-free high-strain single-crystal piezoelectrics in the alkaline–bismuth–titanate perovskite family, Applied Physics Letters 73 (1998) 3683–3685.
[6] M.L. Zhao, C.L. Wang, J.F. Wang, H.C. Chen, W.L. Zhong, Enhanced piezoelectric properties of $(Bi_{0.5}Na_{0.5})_{1-x}Ba_xTiO_3$ lead-free ceramics by sol–gel method, Acta Physica Sinica 53 (2004) 2357–2362.
[7] Y.P. Guo, D. Akai, K. Sawada, M. Ishida, Dielectric and ferroelectric properties of highly (1 0 0)-oriented $(Na_{0.5}Bi_{0.5})_{0.94}Ba_{0.06}TiO_3$ thin films grown on $LaNiO_3$/γ-Al_2O_3/Si substrates by chemical solution deposition, Solid State Sciences 10 (2008) 928–933.
[8] Y.P. Guo, K. Suzuki, K. Nishizawa, T. Miki, K. Kato, Dielectric and piezoelectric properties of highly (1 0 0)-oriented $BaTiO_3$ thin film grown on a Pt/TiO_x/SiO_2/Si substrate using $LaNiO_3$ as a buffer layer, Journal of Crystal Growth 284 (2005) 190–196.
[9] S. Yamazoe, Y. Miyoshi, K. Komaki, H. Adachi, T. Wada, Ferroelectric properties of $(Na_{0.5}K_{0.5})NbO_3$-based thin films deposited on Pt/(0 0 1)MgO substrate by pulsed laser deposition with $NaNbO_3$ buffer layer, Japanese Journal of Applied Physics 48 (2009) 09KA13.
[10] F.K. Lotgering, Topotactical reactions with ferrimagnetic oxides having hexagonal crystal structures-I, Journal of Inorganic and Nuclear Chemistry 9 (1959) 113–123.
[11] W.J. Merz, The electric and optical behavior of $BaTiO_3$ single-domain crystals, Physical Review 76 (1949) 1221–1225.
[12] D.Z. Zhang, X.J. Zheng, X. Feng, T. Zhang, J. Sun, S.H. Dai, L.J. Gong, Y.Q. Gong, L. He, Z. Zhu, J. Huang, X. Xu, Ferro-piezoelectric properties of $0.94(Na_{0.5}Bi_{0.5})TiO_3$–$0.06BaTiO_3$ thin film prepared by metal-organic decomposition, Journal of Alloys and Compounds (2008), doi:10.1016/j.jallcom.2010.05.069.
[13] Z.H. Zhou, J.M. Xue, W.Z. Li, J. Wang, H. Zhu, J.M. Miao, Ferroelectric and electric behavior of $(Na_{0.5}Bi_{0.5})TiO_3$ thin films, Applied Physics Letters 85 (2004) 804–806.
[14] X.J. Zheng, W.M. Yi, Y.Q. Chen, Q.Y. Wu, L. He, The effects of annealing temperature on the properties of $Bi_{3.15}Nd_{0.85}Ti_3O_{12}$ thin films, Scripta Materialia 57 (2007) 675–678.